Electroformation of Giant Unilamellar Vesicles: Investigating Vesicle Fusion versus Bulge Merging

Yasmine Miguel Serafini Micheletto,[†,‡] Carlos M. Marques,[†] Nádya Pesce da Silveira,[‡] and André P. Schroder*,[†]

[†]Institut Charles Sadron, Université de Strasbourg, UPR22-CNRS, 23 rue du Loess, 67034 Strasbourg, France
[‡]Programa de Pós-Graduação em Química, Instituto de Química, Universidade Federal do Rio Grande do Sul, Porto Alegre 90040-060, Brazil

Ⓢ *Supporting Information*

ABSTRACT: Partially ordered stacks of phospholipid bilayers on a flat substrate can be obtained by the evaporation of a spread droplet of phospholipid-in-chloroform solution. When exposed to an aqueous buffer, numerous micrometric buds populate the bilayers, grow in size over minutes, and eventually detach, forming the so-called liposomes or vesicles. While observation of vesicle growth from a hydrated lipid film under an optical microscope suggests numerous events of vesicle fusion, there is little experimental evidence for discriminating between merging of connected buds, i.e., a shape trans- formation that does not imply bilayer fusion and real membrane fusion. Here, we use electroformation to grow giant unilamellar vesicles (GUVs) from a stack of lipids in a buffer containing either (i) nanometric liposomes or (ii) previously prepared GUVs. By combining different fluorescent labels of the lipids in the substrate and in the solution, and by performing a fluorescence analysis of the resulting GUVs, we clearly demonstrate that merging of bulges is the essential pathway for vesicle growth in electroformation.
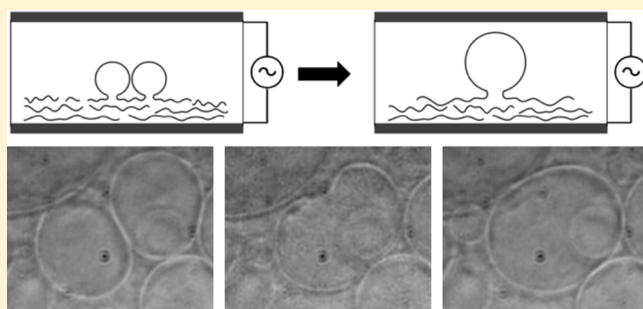
INTRODUCTION

Phospholipid bilayers are model, biomimetic cell membranes. They are often used and studied in the form of unilamellar capsules, named liposomes or vesicles, being most generally suspended in a sugar solution or in a salted buffer.[1−3] It is known that both multilamellar and unilamellar vesicles grow spontaneously from a multilamellar stack of lipids immersed in an aqueous buffer, provided that lipids are in the fluid phase. Observation under an optical microscope shows that since the first moments of its immersion, such a lipid stack starts to swell while its constitutive bilayers assume micrometer scale thermal fluctuations.[3] From then on, numerous round and elongated membrane buds form that grow from submicrometer size to tens of micrometer size and detach eventually from the underlying stack, closing into individual vesicles.

Giant unilamellar vesicles (GUVs) are widely appreciated for model, individual membrane investigations since they are easy to handle and to observe by means of optical microscopy.[4] GUVs can be formed using various techniques, among which are the previously cited spontaneous growth method[5,6] or energy-driven methods such as the well-known electro- formation method.[7] In the latter, a hydrated preformed lipid stack is submitted to an ac field that induces the oscillating motion of the whole lipid stack due to the electro-osmotic behavior of the medium.[8] This results in a decrease of both the surface and line tensions of the swollen bilayers, increasing

bilayer separation and bending.[5,8,9] It is generally admitted that, as compared to spontaneous growth, electroformation presents some advantages, among which are high yields of giant vesicle formation,[10] fewer membrane defects, and high unilamellarity. Although several explanations have been proposed in the past,[11] the mechanisms under which vesicles grow, possibly fuse, and finally detach during electroformation remain a matter of investigation.[10−13]

The present study focuses on the origin of the fusion-like events, such as the one shown in Figure 1a (see also Figure 2 of ref 12 and Movies M1 and M2 in the Supporting Information), that can frequently be observed during any electroformation growth process, while they rarely appear during GUV spontaneous growth. More precisely, the study intends to elucidate if events such as that seen in Figure 1a imply connected buds as schematically depicted by path p1 in Figure 1, which links the initial state (Figure 1b) to the final one (Figure 1e), or correspond to membrane fusion, i.e., involving two independent bilayers that are brought into a close enough contact, as schematically shown by paths p2 and p3 in Figure 1.

Vesicle and liposome dispersions are not thermodynamically stable.[14] However, spontaneous fusion between liposomes
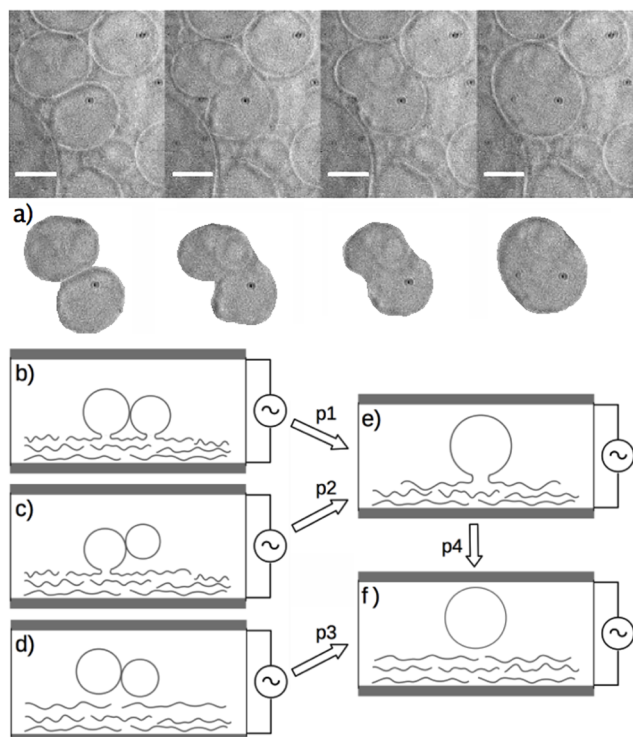
Figure 1. (a) Upper part: phase contrast images showing a typical "apparent" vesicle fusion event during electroformation (see similar fusion events in Movies M1 and M2 in the Supporting Information). Lower part: the two "fusing" vesicles have been extracted by hand deciphering for better visualization. The scale bars represent 10 μm, and the time interval between two consecutive images is 0.73 s. Bud merging, i.e., involving a unique continuous membrane, corresponds to pathway p1. Membrane fusion corresponds to pathway p2 or p3. The pathway (c) → (f) is not considered here, since it involves two elementary steps. Pathway p4 corresponds to the GUV detachment from the underlying lipid stack, not studied in this investigation.

made of neutral, zwitterionic lipids can be considered as negligible over time scales of hours, i.e., the time scale of GUV electroformation. For example, gel-phase vesicles, which miss the repulsive forces that characterize the membrane undulation in fluid-phase liposomes, are known to be unstable and to precipitate over a time scale of days.[15] Also, when submitted to out of equilibrium conditions such as salt misbalance between their interior and exterior, SUVs experience a decrease in their radius due to osmotic forces, but do not fuse.[16] Finally, it is only when neutral, fluid SUVs are submitted to specific conditions that not only force a close contact between neighboring bilayers, but also remove the water molecules that hydrate the phospholipid heads, as, for example, under drying, that they experience membrane fusion.[17]

Clearly, optical techniques alone cannot determine if electroformation induces some membrane fusion during GUV growth. Indeed, images like the one shown in Figure 1a do not allow us to differentiate between bud merging and membrane fusion, since transmission (or fluorescence) microscopy allows only for the visualization of a vesicle or a bud at its equatorial plane. Confocal imaging could circumvent this limitation by its ability to build 3D images. As an example, Figure S4, Supporting Information, in the paper of Yang et al.[18] shows nicely how GUVs can be imaged during growth, using the Z-scan function of a laser confocal microscope. However, the very first moments of the GUV "fusion" process take place over

times shorter than one-tenth of a second (see movies M1 and M2 in the Supporting Information), i.e., much faster than the typical image acquisition duration of a traditional confocal microscope. Even nowadays rapid confocal acquisition devices might be too slow or simply lack optical resolution (due to the diffraction limit) to evidence the exact pathway followed by 4 nm thick membranes during such apparent fusion. To our knowledge, there is no study that precisely describes, using current fast 3D imaging, the growth of vesicles from an underlying lipid stack, as to definitely clarify which pathways lead to the observed vesicle fusion (Figure 1a).

To circumvent optical microscopy limitations due to the 2D observation of a 3D process such as the one evoked here, we study GUV electroformation from preordered lipid stacks in the presence of previously formed giant vesicles or submicrometer liposomes. Differently labeling the underlying stack and the first-generation, suspended vesicles is used to evaluate, from image analysis of the final GUVs, to which extent the previously formed GUVs or liposomes (first-generation) fuse with growing buds or vesicles. As a complement, we check, using dynamic light scattering, if submicrometer liposomes experience fusion when submitted to an electric alternate field such as that applied during the electroformation process.

EXPERIMENTAL SECTION

Materials. The lipids 1,2-dielaidoyl-*sn*-glycero-3-phosphocholine (DEPC; >99%), 1,2-dilauroyl-*sn*-glycero-3-phosphocholine (DLPC; >99%), 1,2-ditridecanoyl-*sn*-glycero-3-phosphocholine (13PC; >99%), 1,2-dimyristoyl-*sn*-glycero-3-phosphocholine (DMPC; >99%), and 1,2-dipentadecanoyl-*sn*-glycero-3-phosphocholine (15PC; >99%) were purchased from Avanti Polar Lipids, in the form of chloroform solutions. The lipid 1,2-dioleoyl-*sn*-glycero-3-phosphocholine (DOPC; >99%) was purchased as a powder from Sigma-Aldrich and dissolved in chloroform. Two fluorescently labeled lipids were also used, 1,2-dioleoyl-*sn*-glycero-3-phosphoethanolamine-*N*-(lissaminerhodamine B sulfonyl) (ammonium salt) (LRhod-PE; >99%) and 1,2-dioleoyl-*sn*-glycero-3-phosphoethanolamine-*N*-(7-nitro-2,1,3-benzoxadiazol-4-yl) (ammonium salt) (NBD-PE; >99%), also purchased from Avanti. Lipid solutions were stored at −20 °C. All the lipids were used without purification.

LUV Formation. Small unilamellar vesicles (LUVs) were prepared as follows: A 1 mL portion of a given lipid in chloroform (1 mg·mL⁻¹) containing a small fraction of fluorescent lipid (0.5%, mol/mol) was inserted into a glass vial. Chloroform was first evaporated under a N₂ flow, and the vial was then placed under vacuum for at least 30 min. The dry lipid film was then hydrated with a 0.2 M sucrose solution under gentle agitation. As a result, an opalescent suspension of multilamellar micrometer-sized vesicles was obtained and was extruded (21 times) through a 100 nm polycarbonate membrane using an Avanti Polar Lipids (United States) extruder. LUV suspensions were stored at 4 °C for further use.

GUV Formation: Electroformation Method. Giant unilamellar vesicles (GUVs) were grown following the electroformation method described by Angelova et al.[7] We differentiate here between the so-called "first-generation" GUVs, which were grown in an aqueous sugar solution, and the "second-generation" GUVs, which were grown in a suspension of pre-existing GUVs or LUVs as explained below.

Growth of First-Generation GUVs. A 10 μL volume of a 1 mg·mL⁻¹ lipid in chloroform solution, containing a small fraction of fluorescent lipid (0.5%, mol/mol), was spread gently with a syringe on the conductive side of two indium tin oxide (ITO)-covered glass slides (PGO, Iserlohn, Germany). Chloroform was evaporated under vacuum for at least 30 min. The two ITO slides were then positioned to form a 2 mm thick electroformation growth chamber (Teflon spacer), their conductive sides facing each other. The chamber was filled with a 0.2 M sucrose solution, and vesicle growth was achieved by applying an ac voltage, 1 V and 10 Hz, for 3 h. The GUVs were
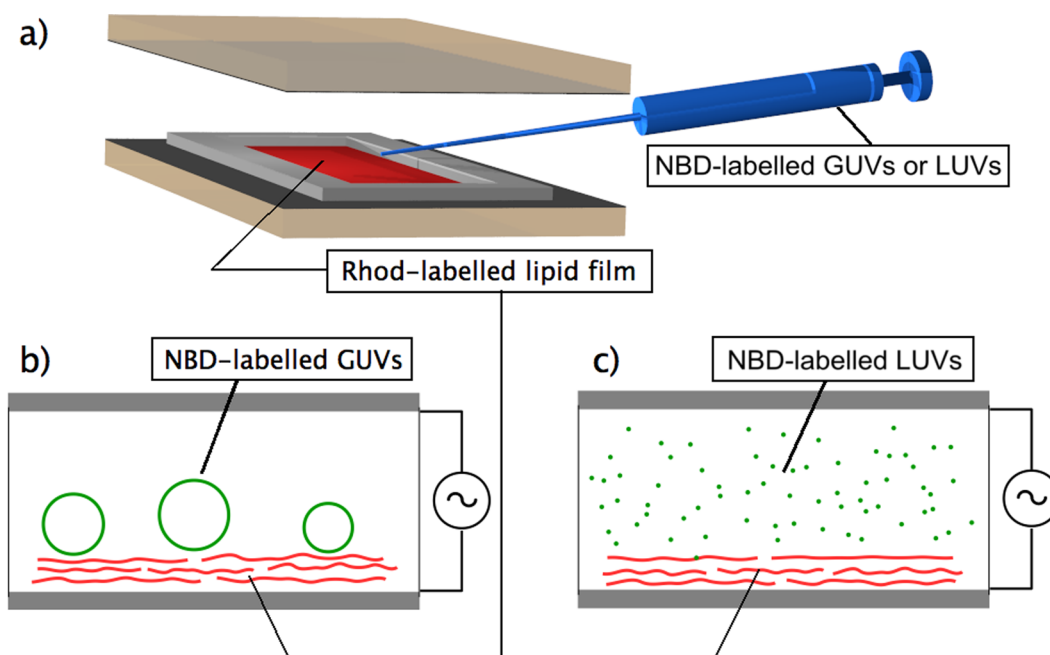
Figure 2. (a) Preparation of the electroformation cell for growing second-generation GUVs: The fluorescently labeled lipid LRhod-PE is first spread onto the ITO-covered, bottom glass slide of the growth chamber. The chamber is then filled with NBD-PE-labeled GUVs or NBD-PE-labeled LUVs. All components are at 4 °C. (b) Starting point for GUVs/w/GUVs growth: First-generation GUVs are allowed to sediment before the alternate voltage is applied while the cell is gently brought to room temperature (50 °C for 15-PC). (c) GUVs/w/LUVs electroformation.

then transferred into a vial and diluted (ca. 2×) in a 0.2 M glucose solution. Due to the density difference between the inner sucrose and the outer glucose + sucrose solutions, the GUVs quickly sedimented under gravity. Osmolarities of both sucrose and glucose solutions were previously finely matched using a cryoscopic osmometer (Osmomat 030, Gonotec, Berlin, Germany). The GUV suspensions were kept at 4 °C for further use, within less than 24 h.

Growth of GUVs in the Presence of GUVs or LUVs. This method implied as a first step the preparation of fluorescently labeled GUVs and LUVs as described above. Each of these first-generation suspensions was collected in a syringe and kept at 4 °C (as explained above, the GUVs were diluted, ca. 1/1, v/v, into an iso-osmolar glucose solution). For simplicity we mostly labeled first-generation GUVs and LUVs with NBD-PE. The lipid LRhod-PE was spread onto an ITO glass, and a growth cell was prepared, as described above. Growth of GUVs in the presence of GUVs was achieved as follows: First, both the growth chamber with the spread lipid and the syringe with the suspension containing the first-generation GUVs were kept at 4 °C for 2 h. Then the growth chamber was filled with the syringe content and kept at 4 °C overnight (Figure 2a). This procedure was adopted to ensure that the first-generation GUVs sediment onto the lipid stack. Finally, the growth cell was brought to room temperature and immediately connected to the ac electric field, followed by the previously depicted electroformation protocol (Figure 2b), except in the case of 15-PC, for which growth was achieved at 50 °C. After 3 h, the vesicles were collected in an Eppendorf vial containing a 0.2 M glucose solution (ca. 1/1, v/v, dilution). In the following, GUVs collected from such a "second-generation" growth process are named GUVs/w/GUVs. We also grew second-generation GUVs in the presence of LUVs. Though this process did not require any latency period for LUVs to sediment after their introduction into the second-generation growth cell, since these small Brownian objects fill the space homogeneously, we however followed the same protocol as for the GUVs/w/GUVs growth, for exact comparison between the two growth methods. GUVs collected from this method are named in the following as GUVs/w/LUVs.

As mentioned above, we present here results with first-generation GUVs or LUVs labeled with NBD-PE, but we also checked that inverting the probes, i.e., labeling first-generation GUVs or LUVs with LRhod-PE, did not modify the experimental conclusions.

Dynamic Light Scattering. Dynamic light scattering (DLS) measurements were performed in a Malvern ZetaSizer Nano ZS apparatus, with a HeNe (633 nm) laser. First, the hydrodynamic diameter d_H of extruded DOPC and DLPC liposomes was measured. Each liposome suspension was then introduced into an electroformation chamber (see above), but in the absence of any spread lipid film on the ITO glass surface. The cell was then submitted to an electric field for 3 h, as for normal electroformation (see above). Finally, the liposome suspension was transferred into a DLS cuvette, and the average size of the liposomes was again measured.

Optical Microscopy. We used an inverted TE 2000 microscope (Nikon, Japan), equipped with a 60× water immersion, 1.2 NA Plan Apo DIC objective and a 40× phase contrast, 0.60 NA Plan Fluor objective. When necessary, epifluorescence images of the GUVs were recorded using a digital camera (Hamamatsu EM-CCD, Japan) with a pixel depth of 16 bits. Most often three-dimensional (3D) fluorescence imaging was performed using confocal laser scanning microscopy (CLSM) with a Nikon C1 scanhead installed on the microscope. Images were then captured using the EZ-C1 software (Nikon, version 3.50). GUVs were systematically imaged using multiwavelength imaging, following the so-called frame λ method (Nikon EZ-C1 software). The method is a wavelength sequential scan, during which the sample is first excited at 488 nm (argon ion laser, Melles-Griot), and second excited at 543 nm (helium−neon laser, Melles-Griot). Confocal images were recorded in the 500−530 nm (respectively 552−617 nm) range when exciting at 488 nm (respectively 543 nm). In the following, these excitation/emission conditions will be referred to as 488/515 and 543/585, respectively. NBD (rhodamine)-containing GUVs showed emitted light only in the 488/515 (543/585) conditions, respectively, while GUVs containing both probes showed emission in both imaging conditions. All confocal images were taken with a unique set of the following parameters: laser power (one specific power for each of the excitation wavelengths mentioned above), PMT amplification (one specific gain for each of the two emission wavelength ranges mentioned above), pinhole size, pixel dwell, image size, and number of pixels per image. Therefore, quantitative comparison in terms of fluorescence emission intensity

C

between images could be performed throughout the whole study. Images were analyzed using homemade software.

Fluorescence Calibration. We first measured the amount of fluorescence detected from bilayers containing known amounts of one or two probes. GUVs were imaged at their equator, always using the same set of confocal settings, as explained above: for each GUV we integrated the absolute fluorescence intensity along the GUV perimeter and than normalized it by the perimeter, obtaining an average fluorescence intensity per pixel length of membrane. The results of our calibration experiments are given in Table 1.

Table 1. Fluorescence Amount per Unit Membrane Pixel Length, Relative Units with Respect to the Pixel Saturation Intensity, As Measured from the Analysis of GUVs Containing 0.5% NBD-PE, 0.5% LRhod-PE, or a 1/1 Mixture of Both Probes (0.25%, mol/mol, Concentration of Each Probe)[a]

|	fluorescence per pixel (fraction of max intensity)	
	488/515 nm	543/585 nm
0.5% NBD-PE	0.20 ± 0.01	no emission
0.5% LRhod-PE	no emission	0.71 ± 0.05
0.25% NBD-PE + 0.25% LRhod-PE	0.091 ± 0.015 (46 ± 8%)	0.315 ± 0.015 (44 ± 8%)

[a]Here results for GUVs of DEPC are given, but similar results were obtained for DOPC. In the parentheses is given the fraction of probe in the membrane relative to the reference probe concentration, i.e., 0.5%, mol/mol, as deduced from the fluorescence intensity (a value of 50% is expected here).

We first quantified the fluorescence of DOPC and DEPC GUVs containing 0.5%, mol/mol, NBD-PE or 0.5%, mol/mol, LRhod-PE (so-called "one-probe" calibration). Each reported value in Table 1 is an average over ca. 20 GUVs for each probe. Data for DEPC and DOPC GUVs are similar. Table 1 shows results obtained for DEPC. The intensity value per pixel is expressed as a fraction of the maximum possible intensity (pixel saturation).

We also measured the fluorescence of GUVs containing a 1/1 mixture of both probes, i.e., 0.25%, mol/mol, NBD-PE and 0.25%, mol/mol, LRhod-PE (so-called "two-probe" calibration). The average intensity per pixel for each emission wavelength should in this case be half of its corresponding value in the "one-probe" condition, as long as there is a linear relation between the measured fluorescence intensity per unit membrane area and the probe concentration in the membrane. Table 1 shows that this condition is fulfilled with an error of 8%.

■ RESULTS AND DISCUSSION

The set of lipids explored in this study was chosen to include both unsaturated and saturated lipids, all of them being zwitterionic. DOPC and DEPC are composed of two 18-carbon chains with one unsaturation per chain. They are thus very close in terms of molecular structure, differing in their main transition temperature T_m, i.e., the temperature below which the membrane is in the gel phase. As explained in the Experimental Section, the growth chamber containing the red-labeled, spread lipid film is filled at 4 °C with a dispersion containing first-generation, green-labeled GUVs, which are allowed to sediment overnight. Thus, this stage of the second-generation growth process occurs in the fluid phase for DOPC,
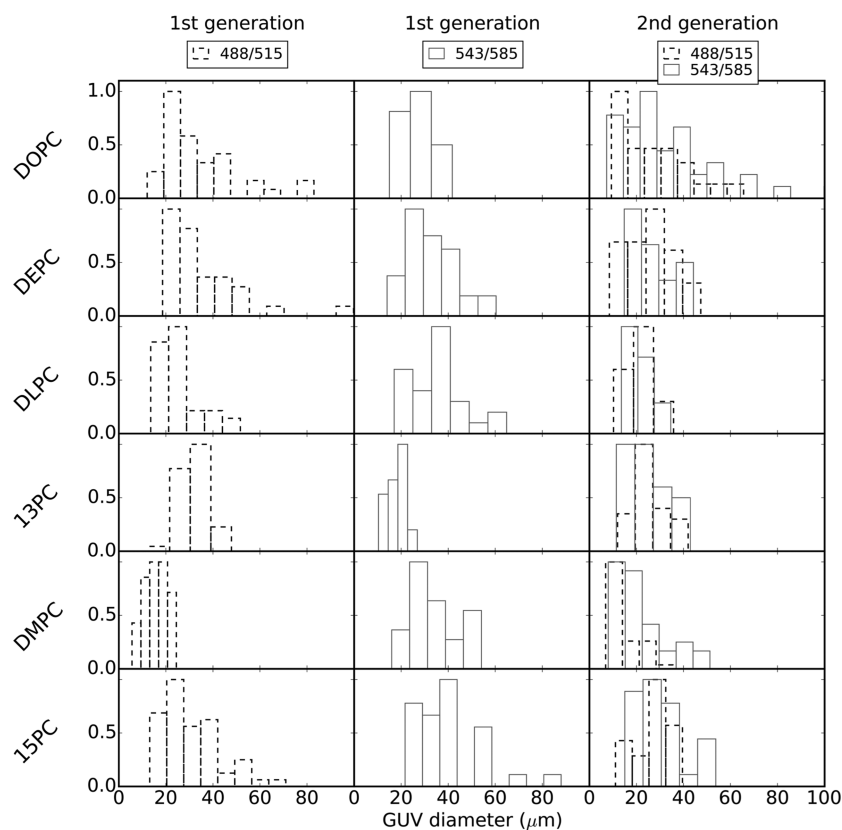
Figure 3. Normalized diameter histograms of GUVs. Left and center columns: GUVs grown using the traditional electroformation method, designed in this paper as "first-generation" GUVs. Green GUVs (488/515) incorporate 0.5%, mol/mol, NBD-PE lipid, and red GUVs (543/585) incorporate 0.5%, mol/mol, LRhod-PE lipid. The right column concerns GUVs/w/GUVs growth, i.e., the content of a "second-generation" growth cell, in which LRhod-PE GUVs were electroformed in the presence of "first-generation" NBD-PE GUVs (see the text for the method).

while it takes place in the gel phase for DEPC. As a result, DOPC experienced spontaneous growth of red GUVs, while DEPC did not, prior to the electroformation stage. Comparing the results between these two lipids aims thus to identify a possible role of spontaneous growth on electroformation. The other lipids are saturated lipids. Hence, a comparison with the two former lipids intends to establish a possible role of unsaturations on electroformation-induced membrane fusion, while comparison between the saturated lipids intends to clarify the role of the chain length on this phenomenon. Again, the set of saturated lipids chosen here contains one lipid with a T_m value lower than the storage temperature (DLPC) to check the possible role of spontaneous growth in the final result. Please note that the T_m of DMPC is very close to room temperature, at which growth was achieved, while the T_m of 15-PC is higher than room temperature, so we electroformed 15-PC GUVs at a higher temperature; here we worked at 50 °C.

Size Distribution of First-Generation GUVs. First-generation GUVs were grown that contained a 0.5%, mol/mol, concentration of fluorescent probe NBD-PE or LRhod-PE, following the procedure described above. We built diameter histograms of the GUVs transferred from the growth cell to an observation cell (Figure 3, left and center columns). In agreement with previous results from the broad literature that exists in the field, GUVs obtained by electroformation were often unilamellar, exhibiting a relatively broad size distribution; here we obtain a distribution of 28 ± 10 μm for the GUV diameter (Figure 3). We argue that the size distribution of our GUVs does not depend on the lipid species. Indeed, though some differences between the histograms might confuse the reader in Figure 3, such as, for example, the coincidence of a lower average value and a narrow histogram for NBD-PE DMPC or LRhod-PE 13-PC or, on the contrary, a broader histogram for NBD-PE DOPC or Rhod 15-PC, when compared to the other histograms, none of these characteristics remain on the histogram of the same lipid that contains the other probe.

Growing GUVs in a Solution of GUVs of the Same Lipid. Second-generation GUVs (LRhod-PE-labeled stacks) were grown in the presence of first-generation GUVs (NBD-PE-labeled) of the same lipid (Figure 2b). After the transfer of the final GUVs into an observation chamber (see the Experimental Section), we recorded confocal microscopy images of the samples in both acquisition modes at 488/515 and 543/585 nm. The analysis of these images showed that, for every sample, virtually all GUVs exhibited fluorescence in only one of the "green" or "red" emission channels. In other words, only a *marginal* number of them have fused into green + red GUVs.

To better assess the size distribution of the different vesicle populations, we compare in Figure 3 size histograms of first-generation GUVs (left and center columns) and of GUVs from GUVs/w/GUVs growth (right column). For computing the histograms for GUVs obtained from GUVs/w/GUVs growth, we considered those vesicles (more than 98% in number as discussed below) that showed only "green" or only "red" fluorescence. As the third column of Figure 3 shows, the diameters of these red or green GUVs have sizes and dispersions comparable to those of their first-generation counterparts. We also measured the diameters of the rare GUVs exhibiting fluorescence in both channels; we found that the measured diameters also fall within the previous size ranges. The distribution of these rare events is not shown in the figure

since their total number is too low to build a representative histogram (see the Discussion below). Each growth condition, corresponding to a given lipid and first or second generation, was repeated three times, leading to similar results.

Interestingly, we also found a systematic asymmetry in the total number of "red" GUVs as compared to the "green" GUVs collected after GUVs/w/GUVs growth. Indeed, notwithstanding a strict and careful protocol during our growth experiences, to (i) collect most of the first-generation GUVs thanks to their sedimentation in the storage vial, (ii) reinject all of them into the second-generation growth cell, and (iii) finally collect as many as possible of the GUVs contained in the GUVs/w/GUVs growth cell, the total number of red GUVs is for all lipids systematically lower than that of the green ones, in a red/green proportion of 46/54 to within 10% (see Table 2, column 5).

Table 2. GUVs/w/GUVs Growth [Number of GUVs Collected from a Second-Generation Growth Chamber, Exhibiting Fluorescence Emission of 488/515 Only, 543/585 Only, or Both Modes, i.e., Having Experienced Membrane Fusion between Membranes Containing Different Probes (Figure 1, p2 or p3)] and GUVs/w/LUVs Growth [Number of Green GUVs][a]

	carbon chain length, number of unsaturations	T_m (°C)	GUV growth temp (°C)	number of GUVs in GUVs/w/GUVs (green/red/bicolor)	number of GUVs in GUVs/w/LUVs (green/bicolor)
DOPC	di 18:1, cis	−22	room	241/193/8	158/0
DEPC	di 18:1, trans	12	room	186/152/6	187/0
DLPC	di 12:0	1	room	159/142/2	218/0
13PC	di 13:0	14	room	108/95/1	183/0
DMPC	di 14:0	23	room	137/113/1	204/0
15PC	di 15:0	33	50	173/133/2	164/0

[a]No GUV had a detectable membrane with two colors.

For completeness of our analysis, we also attempted a characterization of the rare events associated with GUVs that display fluorescence in both the red and the green channels. Figure 4 shows typical images of GUVs collected from a second-generation growth cell. As explained above, the large majority is of a unique color, but in the selected examples of Figure 4 we also show some fused vesicles with both colors. By observation of hundreds of GUVs (Table 2), we were able to collect the following statistical data: With f_{GwG} defined as the fraction of GUVs whose membranes contained both red and green probes, with respect to the total number of GUVs in the sample, DOPC and DEPC, i.e., the unsaturated lipids, show the highest value of f_{GwG}; namely, f_{GwG} is lower than 2%, corresponding in practice to very few, i.e., *less than ten vesicles* (Table 2). For the other lipids the fraction of GUVs with two colors is even lower; i.e., $f_{GwG} < 0.5\%$, corresponding on the whole to less than three GUVs (Table 2).

Growing GUVs in a Solution of LUVs of the Same Lipid. GUVs were also grown in the presence of LUVs of the same lipid, for all the lipids listed in the Experimental Section. Figure 5 shows typical confocal images obtained under these growth conditions. It can be seen that some GUVs encapsulate LUVs, while others do not; this does not imply however any modification of the method of analysis of the membrane fluorescence. We analyzed the fluorescence content of the membranes of ca. 200 GUVs per type of lipid. No GUV
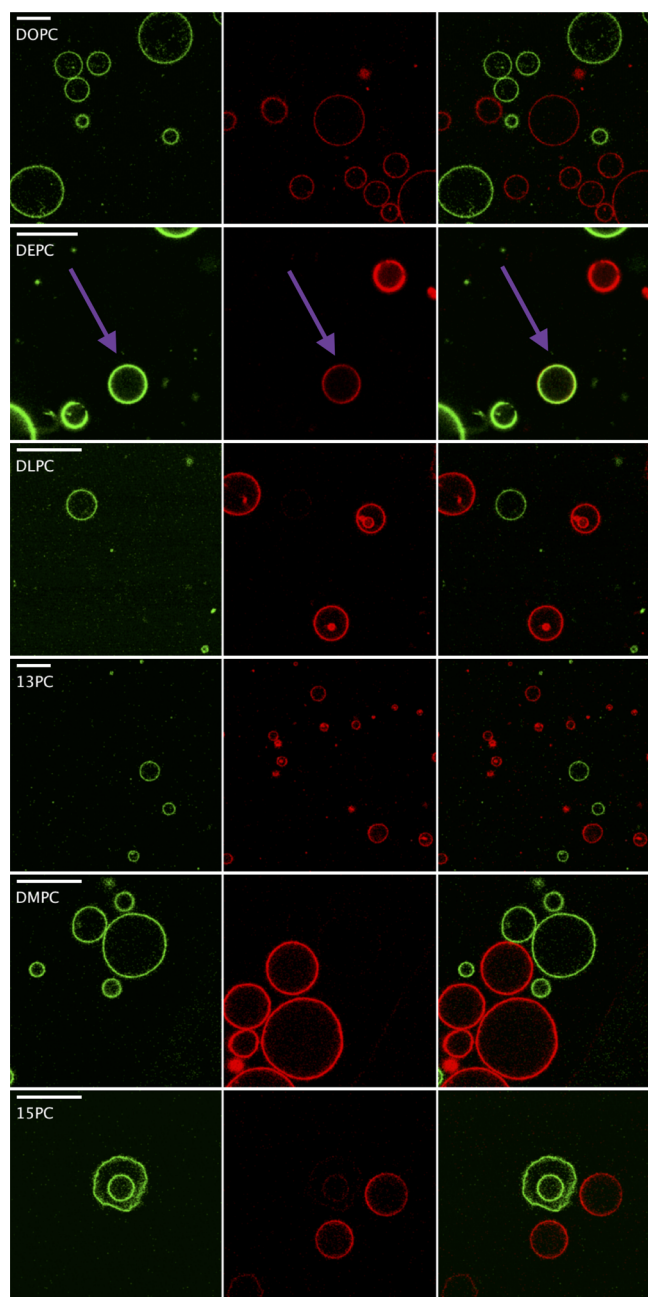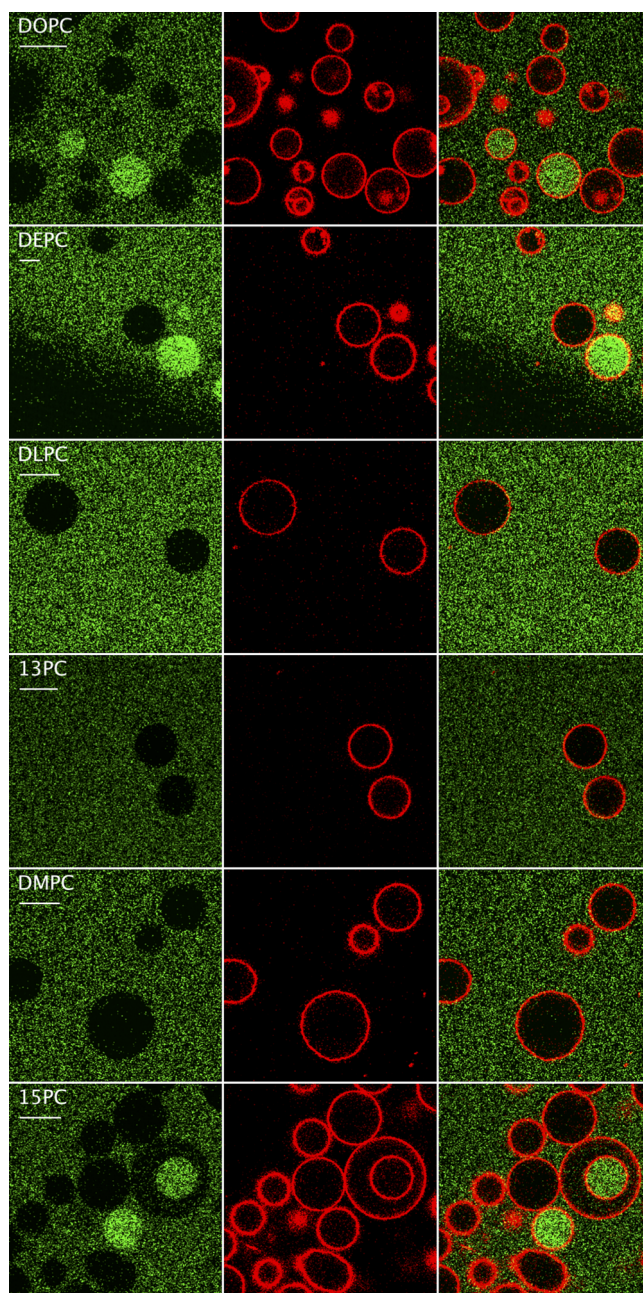
Figure 4. Typical images of GUVs collected from the GUVs/w/GUVs growth method. Left column: 488/515 nm observation. Central column: 543/585 nm observation. Right column: composite image. The scale bars represent 20 μm. The arrow on the DEPC image shows a mixed, "green + red" GUV.

Figure 5. Typical second-generation GUVs from GUVs/w/LUVs electroformation for each lipid used in this study. No membrane contained detectable green fluorescence. The scale bars represent 20 μm.

membrane exhibited any detectable fraction of green color. Therefore, we conclude that no membrane fusion occurred between second-generation, LRhod-PE-labeled GUVs and first-generation, NBD-PE-labeled LUVs. This result is reported in Table 2.

Please note in Figure 5 that GUVs encapsulate different levels of LUVs, as shown by their green fluorescence content. Some of them even exhibit a higher fluorescence than the background. Such results have already been reported and discussed elsewhere.[6]

LUV Behavior under Electroformation Conditions. Finally, the analysis and comparison of the size distribution

of DOPC LUVs on one side, and DLPC LUVs on the other side, show that no fusion occurred when LUVs were submitted to electroformation-like conditions (see the Experimental Section). Indeed, we found d_H = 143 ± 5 nm (d_H = 107 ± 6 nm) for freshly extruded LUVs of DOPC (DLPC), and d_H = 141 ± 6 nm (d_H = 104 ± 4 nm) for the same LUVs after they were submitted to 3 h of electroformation-like conditions.

Discussion. In this work we have produced GUVs by the electroformation technique from a "red-labeled" precursor film of lipid in a growth solution that also contained preformed GUVs or LUVs with "green" labels. The striking outcome of our experiments is that these growth conditions do not lead to any significant amount of GUVs with mixed fluorescent labels,

F

as quantized in Table 2, leading to $f_{GwG} < 2\%$ and $f_{GwL} = 0$. Also, the size distributions shown in Figure 3 are similar for preformed and final green and red vesicles. This points to the absence of fusion phenomena during electroformation, favoring a scenario where vesicle growth proceeds by membrane rearrangement, pathway p1 illustrated in Figure 1. We now critically review this conclusion by considering the outcome of other possible pathways summarized in Figure 1.

We first consider the possible fusion between a red growth vesicle, still connected to the underlying lipid film by a "neck", and a preformed green vesicle, as shown by pathway p2 in Figure 1. If fusion occurred, given the characteristic sizes of the growing buds and vesicles on the order of several micrometers and the typical diffusion coefficients of the lipids in a lipid bilayer on the order of 1 $\mu m^2 \cdot s^{-1}$, one would expect the green lipids to diffuse, during the 3 h of the experiments, into the lipid substrate, thus contaminating the film and the resulting final red vesicles with some diluted amount of green fluorescence. A low amount of green fluorescence in red GUVs from GUVs/w/ GUVs growth was not observed in our case for any of the lipids.

We consider next the possibility of fusion between two vesicles already formed, i.e., not connected by "necks" to the lipid film below, as illustrated by pathway p3 in Figure 1. Let us recall that, at time zero, all the vesicles already formed are green-labeled. The vesicles that grow, detach from the film, and appear in the population that we are now considering are red-labeled. Obviously, the fusion events between any of the vesicles from such a population should lead to (i) pure green vesicles from green–green fusion, (ii) pure red vesicles from red–red fusion, and (iii) vesicles with mixed green and red colors from a green–red fusion, the fractions of each color being proportional to the relative areas of the two merged vesicles. The quantity f_{GwG}, i.e., the fraction of mixed, "green + red"-labeled GUVs in the final population, is thus, under fusion pathway p3, expected to be a function of the relative importance of each of these events, of the size distribution, and of the number and sequence of the fusion events. Although precise predictions for f_{GwG} values under such a scenario are beyond the scope of our analysis, it is straightforward to predict some limiting situations. For instance, if detachment is fast compared to fusion, and if only one fusion event occurs on average per vesicle, one expects $f_{GwG} \approx 0.5$; that is, about half of the vesicle population is expected to contain mixed colors. Larger f_{GwG} values are of course to be expected if a vesicle undergoes several fusion events. If detachment is slow and only one fusion occurs per vesicle, f_{GwG} will be reduced by a proportionality factor that depends on the detachment kinetics and that can be easily estimated from the areas under the supposed kinetic detachment curves, for instance, by a factor of 2 for linear kinetics and by a factor of less than 2 for exponential kinetics. Here also, multiple fusion events would lead to an increase of the f_{GwG} values. In any case, pathway p3 is also expected to lead to a significant amount of vesicles with mixed fluorescent labels in the final vesicles, in contradiction with our findings.

Our conclusion that no fusion occurs during electroformation is further supported by two other experiments. First, electroformation from a red-labeled film made in the presence of green LUVs leads to vesicles with no green fluorescence and comparable GUV size distributions of preformed and final vesicles. Second, electroformation does not induce membrane fusion of (i) LUVs of DOPC, i.e., a double, 18-carbon unsaturated lipid, and (ii) LUVs of DLPC,

i.e., the shorter, 12-carbon fully saturated lipid, as shown by DLS experiments. Please note that the latter experiment, which concerns only floating LUVs in electroformation-like conditions, appears as borderline to the present study, justifying that only two characteristic lipids of our lipid series (see the Experimental Section) have been tested here.

■ SUMMARY AND CONCLUSIONS

In the present study we investigated the nature of events leading to GUV growth during electroformation, such as the one shown in Figure 1a. Our results show that these events, which are *generally* referred to in the literature as "fusion events", are in fact bud merging, involving exclusively a rearrangement of the membrane between two neighboring buds without any bilayer fusion, as depicted by pathway p1 in Figure 1. Our results are quite robust with respect to the variation in lipid chemistry. They are valid for the commonly used physicochemical conditions for electroformation.[4] They hold for a variety of lipids with saturated and unsaturated chains, from 12 to 18 carbons per chain, and thus for bilayers of different thicknesses. They also hold for different preparation conditions at which the lipid film spread on the growing surface is exposed to preformed GUVs or LUVs. In particular, no differences were observed when this temperature was changed from values above to values below the main transition temperatures of the lipid membrane, i.e., enabling or not some spontaneous GUV growth to take place before electroformation started. More generally, the method described here, though indirect, appears as an efficient way to check for membrane fusion during various strategies of GUV growth. For example, it has been recently reported that, in the presence of ions (e.g., Ca²⁺), electroformation produces GUVs with a decreased polydispersity. This has been interpreted as the result of the transient accumulation at the water/lipid interface of Ca²⁺, with a resultant spatial-tuned electro-osmotic flow.[19] Applied to such growth conditions, our GUVs/w/GUVs protocol might help to find out whether membrane fusion takes place under such conditions.

Despite their robustness, our conclusions are not based on a direct imaging of the membranes during electroformation. Direct inspection of these mechanisms by 3D imaging of the interfacial lipid structure comprising the substrate films, the buds, and the formed vesicles is likely to become a reality soon, given the pace of developments of fast confocal microscopes. We certainly look forward to the first measurements of this kind, and to a deeper understanding of membrane transformations during electroformation.

■ ASSOCIATED CONTENT

ⓢ Supporting Information

The Supporting Information is available free of charge on the ACS Publications website at DOI: 10.1021/acs.langmuir.6b01679.

> Movie M1 showing typical "fusion-like" events during electroformation at a time interval between succeeding images of 0.73 s (scale bar 10 μm) (AVI)
> Movie M2 showing typical "fusion-like" events during electroformation at a time interval between succeeding images of 0.36 s (scale bar 10 μm) (AVI)

■ AUTHOR INFORMATION

Corresponding Author

*E-mail: andre.schroder@ics-cnrs.unistra.fr.

Notes

The authors declare no competing financial interest.

■ ACKNOWLEDGMENTS

■ REFERENCES

(1) Walde, P.; Cosentino, K.; Engel, H.; Stano, P. Giant Vesicles: Preparations and Applications. *ChemBioChem* **2010**, *11*, 848−865.

(2) Reeves, J. P.; Dowben, R. M. Formation and properties of thin-walled phospholipid vesicles. *J. Cell. Physiol.* **1969**, *73*, 49−60.

(3) Mueller, P.; Chien, T. F.; Rudy, B. Formation and properties of cell-size lipid bilayer vesicles. *Biophys. J.* **1983**, *44*, 375−381.

(4) Dimova, R.; Aranda, S.; Bezlyepkina, N.; Nikolov, V.; Riske, K. A.; Lipowsky, R. A practical guide to giant vesicles. Probing the membrane nanoregime via optical microscopy. *J. Phys.: Condens. Matter* **2006**, *18*, S1151−S1176.

(5) Rodriguez, N.; Pincet, F.; Cribier, S. Giant vesicles formed by gentle hydration and electroformation: A comparison by fluorescence microscopy. *Colloids Surf., B* **2005**, *42*, 125−130.

(6) Weinberger, A.; Tsai, F. C.; Koenderink, G. H.; Schmidt, T. F.; Itri, R.; Meier, W.; Schmatko, T.; Schröder, A.; Marques, C. Gel-assisted formation of giant unilamellar vesicles. *Biophys. J.* **2013**, *105*, 154−164.

(7) Angelova, M. I.; Dimitrov, D. S. Liposome electroformation. *Faraday Discuss. Chem. Soc.* **1986**, *81*, 303−311.

(8) Dimitrov, D. S.; Angelova, M. I. Lipid swelling and liposome formation on solid surfaces in external electric fields. *Prog. Colloid Polym. Sci.* **1987**, *73*, 48−56.

(9) Taylor, P.; Xu, C.; Fletcher, P. D. I.; Paunov, V. N. Fabrication of 2D arrays of giant liposomes on solid substrates by microcontact printing. *Phys. Chem. Chem. Phys.* **2003**, *5*, 4918−4922.

(10) Bagatolli, L. A.; Parasassi, T.; Gratton, E. Giant phospholipid vesicles: comparison among the whole lipid sample characteristics using different preparation methods: A two photon fluorescence microscopy study. *Chem. Phys. Lipids* **2000**, *105*, 135−147.

(11) Angelova, M.; Dimitrov, D. S. A mechanism of liposome electroformation. *Prog. Colloid Polym. Sci.* **1988**, *76*, 59−67.

(12) Kuribayashi, K.; Tresset, G.; Coquet, Ph.; Fujita, H.; Takeuchi, S. Electroformation of giant liposomes in microfluidic channels. *Meas. Sci. Technol.* **2006**, *17*, 3121−3126.

(13) Lecuyer, S.; Fragneto, G.; Charitat, T. Effect of an electric field on a floating lipid bilayer: A neutron reflectivity study. *Eur. Phys. J. E: Soft Matter Biol. Phys.* **2006**, *21*, 153−159.

(14) Lasic, D. D. *Liposomes: From Physics to Applications*; Elsevier: Amsterdam, 1993.

(15) Michel, R.; Plostica, T.; Abezgauz, L.; Danino, D.; Gradzielski, M. Control of the stability and structure of liposomes by means of nanoparticles. *Soft Matter* **2013**, *9*, 4167−4177.

(16) Sabın, J.; Prieto, G.; Ruso, J. M.; Hidalgo-Álvarez, R.; Sarmiento, F. Size and stability of liposomes: A possible role of hydration and osmotic forces. *Eur. Phys. J. E: Soft Matter Biol. Phys.* **2006**, *20*, 401−408.

(17) Bhatia, T.; Husen, P.; Brewer, J.; Bagatolli, L. A.; Hansen, P. L.; Ipsen, J. H.; Mouritsen, O. G. Preparing giant unilamellar vesicles (GUVs) of complex lipid mixtures on demand: Mixing small unilamellar vesicles of compositionally heterogeneous mixtures. *Biochim. Biophys. Acta, Biomembr.* **2015**, *1848*, 3175−3180.

(18) Yang, P.; Lipowsky, R.; Dimova, R. Nanoparticle Formation in Giant Vesicles: Synthesis in Biomimetic Compartments. *Small* **2009**, *5*, 2033−2037.

(19) Tao, F.; Yang, P. Ca-Mediated Electroformation of Cell-Sized Lipid Vesicles. *Sci. Rep.* **2015**, *5*, 9839.